PRIMA DDL & AOS Project

ARC
EPFL
ASTRON
MPIA Heidelberg
Observatoire de Genève
University of Leiden/NOVA

Astrometric Survey for Extra-Solar Planets with PRIMA

Requirements on Medium-Term Stability of Air Parameters in VLTI Ducts and Delay Lines

Doc. No. VLT-SPE-AOS-15753-0003
Issue 0.2.172
Date June 21, 2006

Prepared	Richard J. Mathar	June 21, 2006	
			Signature
Approved	Denis Mégevand	June 21, 2006	
			Signature
Released	Didier Queloz	June 21, 2006	
			Signature

This page was intentionally left almost blank

Change Record

Issue	Date	Section/Parag. affected	Reason/Initiation/Documents/Remarks
0.1	07-Jul-2005	all	created
0.1.194	13-Jul-2005	Section 5.2	added
0.1.195	14-Jul-2005	Section 6, Ref [5]	added
0.1.206	25-Jul-2005	Section 7.2	added
0.1.291	18-Oct-2005	all	updated references to current [10, 14]
0.1.321	17-Nov-2005	Ref. [9]	changed document number
0.2.172	21-Jun-2006	all	updated references to current [10, 11, 14]

This page was intentionally left almost blank

1 Abstract

Astrometry with PRIMA/VLTI puts high requirements on the knowledge of 4-way, dual-beam differential optical path differences for off-axis beams impinging on two Auxiliary Telescopes. The DRS needs accurate estimates of the refractive index of the air in the ducts, main delay line tunnel and interferometric laboratory to convert phase measurements to "vacuum" delays attributed to the beams above the atmosphere. The dependence of the refractive index on wavenumber and air composition leads to requirements on the knowledge and/or control of temperature, pressure and humidity.

In fulfillment of the PDR AI #2 [2], the requirements are summarized here. This document is not covered by the SOW [1].

1.1 Documents

[1] Delplancke, F. 2004, SoW for PRIMA Astrometric Operations and Software. VLT-SOW-ESO-15750-3298

[2] — 2005, Minutes of Meeting, PAOS Preliminary Design Review. TSD-05/42

[3] — 2005, PRIMA Astrometric Instrument, Template Reference Guide. VLT-TRE-ESO-15750-3669

[4] — 2005, Prima Differential Delay Line (DDL), Performance & Technical Requirement Specifications. VLT-SPE-ESO-15720-2209

[5] Delplancke, F., Lévêque, S., Kervella, P., Glindemann, A., & d'Arcio, L. 2000, in Interferometry in Optical Astronomy, edited by P. J. Lena, & A. Quirrenbach (Int. Soc. Optical Engineering), vol. 4006 of Proc. SPIE, 365

[6] Folco, E. D., & Koehler, B. 2002, VLTI Commissioning Part I: OPD stability, Test Report. VLT-TRE-ESO-15000-2902

[7] Glindemann, A. 2000, PRIMA, the Phase Referenced Imaging and Microarcsecond Astrometry facility: System Description. VLT-SPE-ESO-15700-2207

[8] Lévêque, S. 2000, Results of environmental tests for the VLTI at Paranal, May 11–21/00. VLT-TRE-ESO-15000-2259

[9] Mathar, R. J. 2005, Astrometric Survey for Extra-Solar Planets with PRIMA, Requirements on Differential AT Mirror Surface Localizations. VLT-TRE-AOS-15753-0004

[10] — 2006, Astrometric Survey for Extra-Solar Planets with PRIMA, Astrometric dispersion correction. UL-TRE-AOS-15753-0010

[11] — 2006, Astrometric Survey for Extra-Solar Planets with PRIMA, Choice of Detector Spectral Band Widths. UL-TRE-AOS-15753-0012

[12] Peron, M., Wallander, A., Wallace, P., Richichi, A., Ballester, P., Kaufer, A., Percheron, I., Wittkowski, M., Hanuschik, R., Chavan, A. M., & Laing, R. 2005, Astrometric Survey for Extra-Solar Planets with PRIMA, AOS PDR RIX. VLT-SPE-AOS-15750-

[13] Reffert, S., Quirrenbach, A., Jaffe, W. J., & Mathar, R. J. 2005, Astrometric Survey for Extra-Solar Planets with PRIMA, Operation and Calibration Strategy. VLT-TRE-AOS-15754-0001

[14] Tubbs, R. N., & Mathar, R. J. 2006, Astrometric Survey for Extra-Solar Planets with PRIMA, Astrometric Error Budget. VLT-TRE-AOS-15753-0001

1.2 Acronyms

AI Action Item

ARC Ecole d'ingenieurs de l'arc Jurassie `http://www.eiaj.ch/`

ASTRON Stichting Astronomisch Onderzoek in Nederland `http://www.astron.nl`

AT Auxiliary Telescope (of the VLTI) `http://www.eso.org/projects/vlti/AT/index_at.html`

DDL Differential Delay Line `http://www.mpia-hd.mpg.de/PRIMA-DDL/`

DOPD differential OPD

DRS Data Reduction System

EPFL École Polytechnique Fédérale de Lausanne `http://www.epfl.ch`

ESO European Southern Observatory `http://www.eso.org`

FSU Fringe Sensing Unit

MDL main delay line

MPIA Max-Planck Institut für Astronomie, Heidelberg `http://www.mpia.de`

NOVA Nederlandse Onderzoekschool voor Astronomie `http://www.strw.leidenuniv.nl/nova/`

OPD optical path difference

OPL optical path length

PDR Preliminary Design Review

PRIMA Phase-Reference Imaging and Microarcsecond Astrometry `http://obswww.unige.ch/Instruments/PRIMA`

PRIMET PRIMA Metrology `http://www.eso.org/projects/vlti/instru/prima/description_lms_prima.html`

PS primary star

SOW Statement of Work

SS secondary star

UT Unit Telescope (of the VLTI) `http://www.eso.org/projects/vlt/unit-tel/`

VLTI Very Large Telescope Interferometer `http://www.eso.org/vlti`

2 PRIMA Astrometric Mode

The dual-beam interferometer PRIMA at the VLTI aims at μas accuracy for the differential OPD (DOPD) between the two stars/sources. Standard trigonometry for template baselines of ≈ 100 m translates this to requirements on the accuracy of the delay difference between the two interferometers represented by both beams of typically ≈ 5 nm [7]. [1]

The key parameter is the DOPD

$$\Delta D = L_{\mathrm{P1}} - L_{\mathrm{P2}} - (L_{\mathrm{S1}} - L_{\mathrm{S2}}) \tag{1}$$

between star beams P and S from telescopes 1 and 2 to the detectors. It consists of

1. the DOPD within the atmosphere from lensing,[2]
2. concealed contributions from asymmetries within the two AT Coudé trains,[3]
3. the explicit DOPD introduced by the DDL [4], optionally operating in vacuum,[4]
4. the implicit DOPD added by the four (different) refractive indices that convert geometric to optical path differences in Equation (1).

This memorandum deals exclusively with the last item in this list and its role in putting requirements on environmental parameters of the VLTI tunnel.

3 Astrometric Error Budget

In rough terms, PRIMA interferometry senses phases of the two wave packets by the FSUs near their "white light" fringe position, representing the sum of the four paths L itemized in Section 2 that contribute to $L_{\mathrm{P1}} - L_{\mathrm{P2}}$ on one FSU and $L_{\mathrm{S1}} - L_{\mathrm{S2}}$ on the other. Each FSU measures a wrapped phase[5]

$$\varphi(k = K) = n(k)kD_t - kD \tag{2}$$

depending on

- the optical path difference $nD_t = L_1 - L_2$ in the tunnel,
- the "effective" wavenumber k of the starlight,
- and the "external" D above the atmosphere,

where $n(k = K)$ is the K-band refractive index. The DRS—in a differential way—takes these phases, reduces the PRIMET J-band DOPD to measured delay line positions D_t, then combines both to produce D.[6]

Here, we only look at the contribution of the variable n to the error budget, where n depends on

[1] This transformation is detailed in Section 28.3.2 of [14], and not reviewed here.
[2] see Section 5.4 of [10].
[3] Section 11.4.2 of [14] and [9]
[4] see Table 6 of [10]
[5] In terms of radically simplified master equations of Section 6.4 of [10]
[6] Principles of this have been presented in Sections 4.1 and 4.2 of [11]. Use of PRIMET replaces $n(k = K) - 1$ in Equation (2), which is $\approx 2 \cdot 10^{-4}$, effectively by a term $\propto [n(k = K) - n(k = J)]$ which is $\approx -5 \cdot 10^{-7}$. This has been detailed in Section 9 of [14].

1. wavenumber $k = 2\pi\sigma = 2\pi/\lambda$ (band, color)
2. molecular composition of the air, which is a function of
   (a) temperature T
   (b) pressure p
   (c) humidity h

   which all fluctuate as a function of time t and tunnel location x.

The actual fluctuations of these parameters have been characterized in Section 6.1 of [10] and in the documentation listed in Section 23 of [14]; we explicitly do *not* attempt to review the *actual* environmental conditions. To the degree that the consortium has become aware of and actually got hold on documentation, and probably beyond, this information is already in the hands of ESO.

4 Dispersion Effects

4.1 Dispersion Correction

The task of the "dispersion correction" is to keep track of n to reduce the error of the knowledge on the differential nD_t below 5 nm. The dependence of air dispersion on the parameters listed in Section 3 leads to various higher-order differential terms with the potential to introduce errors.[7]

4.1.1 Difference in Beam Dispersion Curves

Virtual rearrangement of Equation (1) as $\Delta D = L_{\mathrm{P1}} - L_{\mathrm{S1}} - (L_{\mathrm{P2}} - L_{\mathrm{S2}})$ shows that the "horizontal" gradients across 24 cm of beam separation remain the dominant contribution of tunnel dispersion to the error budget. Depending on how the beams are organized in the ducts, ie, whether the AT stations are on the same or opposite side of the tunnel, the bias within $L_{\mathrm{P1}} - L_{\mathrm{S1}}$ may have the same or the opposite sign of the bias in $L_{\mathrm{P2}} - L_{\mathrm{S2}}$ [8], which causes the problem to be enhanced $\propto (L_1 + L_2)$, or reduced $\propto |L_1 - L_2|$.

Pairs of consecutive measurements with swapped beams[8] allow to cancel this term computationally during the data reduction by working with the mean of the differential phase, which eliminates the effect to the first-order differentials $\partial n/\partial T$, $\partial n/\partial h$ and $\partial n/\partial p$. Considering the second order partial derivatives leads to the requirements of Section 5.1. The actual time interval between a pair of beam-switched measurements is left as a parameter in the calculation. This time increases if the two configurations are kept apart on the template level [3].

4.1.2 Difference in Mean Star Color

Differences in the effective wavelengths of the two stars introduces two aspects when it comes to reading the two refractive indices off the dispersion curve: Knowledge of the abscissae (ie, the effective wavenumbers), and knowledge of the refractive index at that abscissa. Only the latter belongs in

[7] see Section 9 of [14] and Section 3.2.2 of [10].
[8] Section 6.1 of the PDR documentation [13]

here.[9] The requirements in Section 5.2 follow in straight forward manner by reverse reading of the second table on page 55 of [14].

4.2 Pistonic Fluctuations

Short term "statistical" contributions from density fluctuations [6] within the detector integration time introduce k-dependent Strehl factors (loss of coherence) that modify the effective shape of the K-band spectrum equivalent to a reddening, see Figure 1.[10]

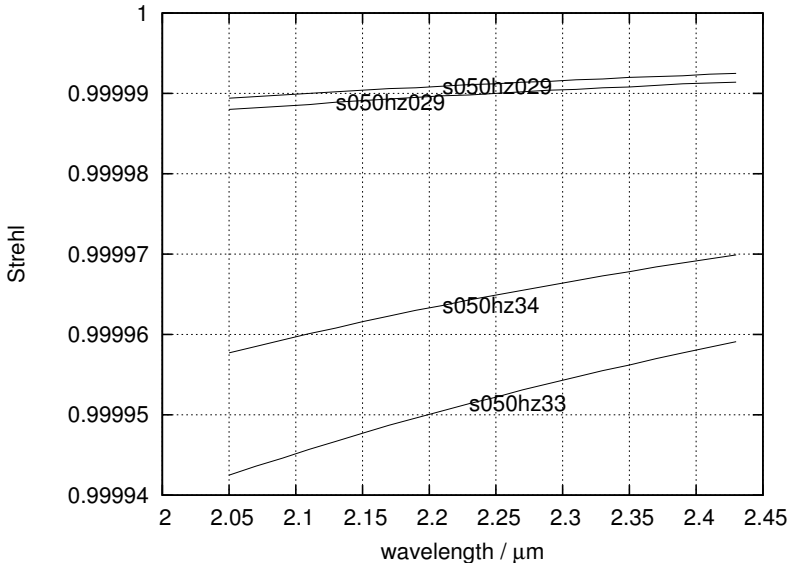

Figure 1: Strehl factor $\exp(-\sigma_\varphi^2/2)$ for four measured OPL fluctuations caused by the UT3 duct [8], assuming a $t = 48$ ms integration time. $\sigma_\varphi = 2\pi\sigma_L/\lambda$ and $\sigma_L \propto t^{3/4}$.

Although the high-frequency reading of PRIMET provides the information to estimate the effect, the high resolution of 11 000 requested for the effective wavenumber[11] might call for frequent re-calibration of the effective K-band spectrum due to changes in the turbulence spectrum of the tunnel.

The signature of this tunnel seeing effect is separable from the atmospheric seeing effect, since it creates a residual pistonic motion of the SS even with perfect tracking of the PS, and limits the integration time also for the SS to increase the effect of readout and photon noise.

This establishes the requirements of Section 5.3.

[9] The star color term listed under the second bullet of item 2 of Section 2 of [14] is off topic in this subsection because it is not correlated to *fluctuations* of the ambient parameters. However, it resurfaces to produce the systematic effect of Section 4.2.

[10] and Section 23.4 of [14]. The same effect is produced by mirror vibrations which show the same chromaticity in the phase and have been measured at 100 nm in the tunnel and 100 nm in one AT arm [12, RIX 003]—which, again, is off-topic here, but means more of these error terms bite off a piece of the same cake.

[11] Equation (34) and Table 1 of [14]. This assumes the layout of the FSU spectral channels as planned.

5 Requirements

5.1 Horizontal Inter-Beam Temperature/Humidity Gradient Drift

The horizontal temperature gradient must change on longer time-scales than needed for the beam swapping. The residual error that would not be removed by the beam swapping technique is proportional to the second derivative of $\partial^2 n/\partial T^2$ multiplied by the half of the product of the inter-beam temperature difference, of the temperature drift during the swap, and of L_1+L_2 (using the pessimistic sign of Section 4.1). More generally, the sum of the contribution of all second order derivatives with respect to the parameters of n must stay below 5 nm. Table 1 shows

- in the first column the pair of variables that could differ between the beams and/or change in time,
- in the second column and third column the typical values of the second derivative and its units,
- and in the last column the allowance in the spatio-temporal product of inter-beam bias and time drift between swaps to keep the error below 5 nm, assuming a typical value of $(L_1+L_2)/2 \approx 180$ m.[12]

2nd derivative		units	product requirement
$\partial^2 n/\partial T^2$	$-1.2 \cdot 10^{-9}$	$1/\mathrm{K}^2$	0.023
$\partial^2 n/\partial h^2$	$-3.3 \cdot 10^{-7}$	$1/(\mathrm{mole/m}^3)^2$	0.000082
$\partial^2 n/\partial p^2$	$-2. \cdot 10^{-14}$	$1/\mathrm{Pa}^2$	1400.
$\partial^2 n/(\partial T \partial h)$	$6.6 \cdot 10^{-7}$	$1/(\mathrm{K\ mole/m}^3)$	0.000042
$\partial^2 n/(\partial T \partial p)$	$-1.4 \cdot 10^{-10}$	$1/(\mathrm{K\ Pa})$	0.20
$\partial^2 n/(\partial h \partial p)$	$1.4 \cdot 10^{-10}$	$1/(\mathrm{mole/m}^3\ \mathrm{Pa})$	0.20

Table 1: Second derivatives of the index of refraction w.r.t. temperature, absolute humidity and air pressure at a wavelength of 2.25 μm, typical values inside the VLTI tunnel.

The way of reading the first line in the table is, for example, that a temperature difference of 0.1 K between the beams can lead to an error of 5 nm if both temperatures drift by 0.23 K during the beam swap, or that a temperature difference of 0.2 K to the same error of 5 nm if both drift by 0.11 K during the swap. The interpretation of the fourth line is, for example, that a temperature difference of 0.1 K allows a drift of absolute humidity of 0.00042 mole/m^3 or that a humidity difference of 0.1 mole/m^3 allows a temperature drift of 0.00042 K (the second interpretation being unrealistic, of course). The sensitivity to the ambient pressure fluctuations is weak.

5.2 Mean Molecular Composition I

The error in the contribution $D\Delta\lambda\frac{\partial n}{\partial k}$ to the DOPD for known effective wavenumber difference Δk of the two stars consists of contributions from temperature fluctuations ΔT and humidity fluctuations Δh according to

$$D\Delta n = D\Delta\sigma\frac{\partial n}{\partial \sigma} + D\Delta\sigma\left(\frac{\partial^2 n}{\partial\sigma\partial T}\Delta T + \frac{\partial^2 n}{\partial\sigma\partial h}\Delta h + \frac{\partial^2 n}{\partial\sigma\partial p}\Delta p\right), \tag{3}$$

[12] taken from Figure 11 of [10]

where $\sigma = 1/\lambda$ with coefficients listed in Table 2.[13]

2nd derivative		units	product requirement
$\partial^2 n/(\partial\sigma\partial T)$	$-3.5 \cdot 10^{-13}$	$1/(\mathrm{cm}^{-1}\ \mathrm{K})$	140.
$\partial^2 n/(\partial\sigma\partial h)$	$1.25 \cdot 10^{-10}$	$1/(\mathrm{cm}^{-1}\ \mathrm{mole/m}^3)$	0.40
$\partial^2 n/(\partial\sigma\partial p)$	$1.3 \cdot 10^{-15}$	$1/(\mathrm{cm}^{-1}\ \mathrm{Pa})$	37000.

Table 2: Second derivatives of the index of refraction w.r.t. spectroscopic wavenumber, temperature, absolute humidity and air pressure at a wavelength of 2.25 μm.

The second term at the r.h.s. of Equation (3) is to be kept smaller than 5 nm at a typical delay of $D = 100$ m, which yields the requirements on the products $\Delta\sigma\Delta T$, $\Delta\sigma\Delta h$ and $\Delta\sigma\Delta p$ which are included in the last column of the table. For a *total* error below 5 nm, the values ought be divided by two—the variation in the pressure is negligible and the error may be shared by the contribution from ΔT and Δh. The transition from different star temperatures to $\Delta\sigma$ is shown with Figure 23 of [11].

Example: For the central spectral channel, $\Delta\sigma$ will hardly ever be larger than 10 cm^{-1} or $\Delta k/k = 1/440$; from the last column in Table 2 one deduces that a combined knowledge of the temperature to 7°C and absolute humidity to 0.02 $\mathrm{mole/m}^3$ suffices to keep the total error below 5 nm.[14] The effective wavenumber of spectral channel in the short-K band, however, is much more sensitive to the star color,[15] rendering a wavenumber difference of 10 cm^{-1} quite plausible; an *independent* DOPD estimate from *this* spectral channel puts more stress on the sensor network.

5.3 Turbulence

To enforce that the decoherencing described in Section 4.2 does not change the effective wavenumber by more than 0.4 cm^{-1} in the central spectral window on behalf of the star color term,[16] the variance σ_L of the differential OPD over the detector integration time interval[17] at the specific star temperature must stay below 66 nm.[18] This effect of turbulence in the ducts implicitly limits the integration time for blind tracking on the SS, for example to 880 ms and 1.1 s for the two measurements `s050hz029` in Table 10 of [8], or to about 300 ms for the more turbulent environment measured under `p050hz10` in Table 16 of [8].

The transition from turbulent to laminar flow in the ducts could be made by reducing the air velocity below (estimated) 0.1 m/s.[19] This would leave only larger convection rolls in the MDL tunnel caused by the vertical temperature gradients, which probably would live on outer scales larger than the inter-beam distance of 24 cm.[20]

[13] At 2.25 μm, $\partial n/\partial\sigma \approx 1.1 \cdot 10^{-10}$ $1/\mathrm{cm}^{-1}$, which can be read from Figures 3, 6 of [10] or 15 of [11]. $\partial^2 n/(\partial\sigma\partial T) \approx -(\partial n/\partial\sigma)/T$ at $T \approx 300$ K as expected from the ideal gas equation.

[14] The humidity bound is usually more difficult to meet than the temperature bounds, and a trade-off can be made.

[15] Bottom of Figure 23 of [11].

[16] listed under the second bullet of item 2 of Section 2 of [14] to keep the error below 5 nm at 100 m OPD. To be devided by $\sqrt{2}$ to account for both stars.

[17] See Figure 2 of [5]

[18] Simulated for black body spectra from 3000 to 12000 K multiplied by the detector quantum efficiency and the Strehl factors as in Figure 1.

[19] see Section B.3 of [14].

[20] This would explain why the DOPD fluctuations in the tunnel have been measured to be much smaller than in the ducts [8]. It also predicts that the conditions in the narrower AT ducts are more turbulent than in the UT ducts.

6 Summary

To define the effective wavenumber of the spectrum to better than 0.4 cm^{-1}, the r.m.s. of the combined turbulence and mirror motions must be smaller than 66 nm if measured over the detector integration time.

The product of the temperature-temperature, humidity-humidity, and temperature-humidity spatio-temporal fluctuations (inter-beam and inter-swap) must each stay below a third of the value listed in Table 1, which are $7.7 \cdot 10^{-3}$ K^2, $2.8 \cdot 10^{-5}$ $\mathrm{mole}^2/\mathrm{m}^6$ and $1.4 \cdot 10^{-5}$ K· $\mathrm{mole}/\mathrm{m}^3$.[21]

7 Appendix

7.1 Horizontal Longitudinal Temperature Gradient

In principle, the single beam baseline calibration to 50 μm accuracy by color calibration of PRIMET puts requirements on the knowledge of the environmental parameters —rather than on the stability/control. We assume the single-channel fringe counters with a resolution of 1.3 μm are available to the DRS. Then the product of the difference between the indices of refraction in the J- and K-band by the OPD must be known to 50 μm. Table 6 of [14] already provides the variation of this factor for 12 cm of OPD. Rescaling leads to the conclusion of Section 3.2.3 of [10] that actually no measurement of T, h or p is needed to achieve the accuracy—using yearly averages is sufficient.

7.2 Mean Molecular Composition II

The two auxiliary spectral channels are potentially useful for fringe tracking, if their phase estimate allows to avoid fringe jumps in the main channel. If we require that fluctuations ΔT and Δh in temperature and humidity do not change the phase difference between the main and a side channel by more than 2π, this confusion limit reads[22]

$$\frac{\partial^2 n}{\partial\sigma\partial T}\Delta T + \frac{\partial^2 n}{\partial\sigma\partial h}\Delta h < \frac{1}{\sigma D\Delta\sigma}, \tag{4}$$

where $\Delta\sigma$ is the difference between the effective wavenumber of the channels, and up to 1300 cm^{-1}.[23] With the derivatives of Table 2, one needs $\Delta T < 50$ K or $\Delta h < 0.14$ $\mathrm{mole}/\mathrm{m}^3$ at $\sigma = 4400$ cm^{-1} and $D = 100$ m to violate the inter-channel phase reference condition (4). These requirements are weaker than those presented in Section 5.2.

___oOo___

[21] This is a combined request to air parameters and speed of execution of the derotator/reaquisition procedure that defines the beam switching technique.

[22] See Section 4.1.2.4 of [11] for a derivation.

[23] See Figure 23 of [11].